Hindawi
Shock and Vibration
Volume 2019, Article ID 4971695, 12 pages
https://doi.org/10.1155/2019/4971695

Research Article

Experimental Study on Acoustic Emission Characteristics of Dry and Saturated Basalt Columnar Joints under Uniaxial Compression and Tensile Damage

Liu Gang[1,2] **Xiao Fu-kun**[2] **Cheng Qian-long**[2] **and Qin Tao**[2]

[1]*Key Laboratory of Safety and High-efficiency Coal Mining, Ministry of Education, Anhui University of Science and Technology, Huainan 232001, China*
[2]*Heilongjiang Ground Pressure & Gas Control in Deep Mining Key Lab, Heilongjiang University of Science & Technology, Haerbin 150022, China*

Correspondence should be addressed to Xiao Fu-kun; xiaofukun@hotmail.com

Received 16 May 2018; Accepted 1 September 2018; Published 6 January 2019

Academic Editor: Daniele Baraldi

An experimental study was carried out to investigate the acoustic emission (AE) characteristics of dry and saturated basalt columnar joints under uniaxial compression and tensile damage by using the TAW-2000 rock experiment system and SH-IIAE system for the whole loading. The results show that the softening coefficient of uniaxial compressive strength and the tensile strength was 0.78 and 0.68, respectively, and water increases the sample complexity and has a strong effect on its strength. The dry sample under uniaxial compression at the beginning of loading produced a large number of AE signals, and the AE signal showed steady growth as the load increased, but the sample destruction occurred during the blank period, which can be used as a precursor of instability. From the amplitude-time-energy diagram, it can be found that as amplitude increases with hit, energy decreases, which shows an obvious triangle relation. From the uniaxial compression damage AE location map, we can find that AE events exist disorderly and show scattered distribution in each area. From the failure modes and sections of tension and uniaxial compression tests, it is found that there are many layers and fissures in rock samples, which are consistent with AE location.

1. Introduction

In the process of underground tunnel excavation, dynamic disasters mainly rock burst and tunnel collapse occur. They are caused mainly by combination of tension and compression stress; the rock tensile strength has far less effect than the compressive strength, but the tensile stress is the primary reason for failure. Due to many disadvantages in direct tensile rock material, an experimental method called the Brazilian splitting method is recognized. Baihetan Hydropower Station was constructed with a cofferdam and a diversion tunnel (Figure 1). While constructing the diversion tunnel, excavation of the surrounding rock revealed a large number of basalt columnar joints in the left and the right bank, and the rock section appears large-area collapse. Diversion tunnel is very important in hydropower construction. The purpose of the diversion tunnel is to divert water, but the diversion of water weakens the rock to a certain extent, which will have an impact on its mechanical properties. During the excavation stage, the basalt columnar joint will be in dry state, and the rock mass will be damaged during excavation and unloading. During the process of water conduction, the basalt columnar joints will get soaked in water for a long time and remain in the state of full water. At this time, the rock mass will be damaged, and it will also be damaged under the action of the external load; hence, the laboratory experiment is the mechanical experiment of the basalt columnar joints conducted under dry and saturated water conditions. This affects the whole project progress speed, so it is very necessary to study the characteristics of basalt columnar joints of the diversion tunnel rock, the nature of which is changed by the running water. AE

Figure 1: Jinsha Jiang crane sketch of basalt columnar joints of Baihetan Hydropower Station and dam.

technology monitors rock mass damage relatively mature, and AE activities responses rock instability and failure. Therefore, this article studies the AE monitoring of the whole process of basalt columnar joints damage to know the characteristic of AE of rock failure process, which provides the theoretical basis for the AE prediction.

Rock instability failure is mainly due to a large number of microcracks convergence, forming macrocracks and penetration leading to fracture. Rock material loading damage is due to the total strain energy accumulation; meanwhile, the form of crack propagation releases elastic wave energy. The AE sensor receives rock energy information which detects internal crack propagation and damage degree. AE monitoring of rock failure process has made many achievements. Li et al. [1] studied the *b*-values and spatial distribution fractal dimension values of AE during uniaxial compression rock failure process. Zhang et al. [2] carried out AE experiments on water-bearing sandstone under uniaxial loading and discussed the changes of natural state, frequency, and energy of water-bearing rock. Liu et al. [3] established AE parameters and damage evolution equation to analyze the relationship between damage and crack propagation. Zhao et al. [4] discussed the rock sample loading damage based on the relationship between sound velocity and AE parameters. Yu et al. [5] used manufacture tensile system that has carried on sandstone and limestone the direct tension to splitting and uniaxial compression damage AE experiment. Zhang et al. [6] performed direct tensile AE experiment on raw coal and discussed the mechanical properties of raw coal and the rule of damage. Li et al. [7] analyzed AE regularity in the failure process under uniaxial compression and splitting test. Fu et al. [8] used rock damage simulation software RFPA splitting the process of stress distribution analysis. Li et al. [9] carried out the combined AE experiment of compression-shear for briquette specimens. Xiao et al. [10, 11] explored uniaxial- and triaxial-type coal AE properties. Zhengwen et al. [12] and Zhang et al. [13] researched on crack propagation and the process of failure precursor information according to the AE based on *b*-value dynamic characteristics and the significance. Tang et al. [14] carried out numerical simulation of AE activities in the process of pillar failure. Wu and Zhao [15] studied the AE characteristics of materials under different stress states. Most scholars [16] discussed deformation experiment of uniaxial compression in order to judge the compressive strength of the stand rock. Few studies on tensile failure have been carried out [17]. The AE technique is suitable to locate the failure positions and determine the energy released in rock failure laboratory experiments due to excavation in mines [18, 19]. The AE and far-infrared (FIR) techniques were applied to monitor the progressive failure of a rock tunnel model subjected to biaxial stresses [20, 21]. The rock tensile properties study AE in the process. It is a helpful method to know the rock failure and for analyzing the stability of surrounding rock AE, which is also very useful. There are only few research studies on physical and mechanical properties of basalt columnar joints; this article investigates the AE monitoring of basalt columnar joints destruction under uniaxial compression and tensile damage experiment. By analyzing the damage situation, AE parameters, and rock's damage AE precursor information, this study provides theoretical support for field monitoring. The stability of columnar jointed basalt in Baihetan Hydropower Station dam area under saturated condition is studied, which can provide some guidance for dam foundation, underground chamber construction, and water-related rock mass engineering problems with abundant columnar jointed basalt.

2. Indoor AE Experiment of Basalt Columnar Joints

2.1. Sample Preparation. The test rock samples were taken from $K_{0+310-K0+325}$ columnar joint development section of No. 3 diversion tunnel of Baihetan Hydropower Station on Jinsha River. First, the rock sample was put on the machine processing platform, and the diamond core drill was used with a 50 mm diameter cylinder, secondly, the same was cut, respectively, into 100 mm and 15~28 mm cylindrical specimens by a stone cutting machine, and finally, the double rock machine grinds flat two end face, thus the required rock sample is obtained. Precision testing requirements are as follows: (1) unparallelism of the maximum and the minimum deviation should be controlled within 0.05 mm. (2) The upper and lower end diameter deviation should not be greater than 0.3 mm. (3) The specimen surface is smooth, and the axial deviation should not be more than 0.25° [22]. Ten specimens of $\Phi 50 \times 100$ mm were processed. Ten specimens of size $\Phi 50 \times 14.8$~27.3 mm were processed.

2.2. Laboratory Equipment. The rock sample was processed under uniaxial compression and splitting AE experiment by using the TAW-2000 microcomputer-controlled electrohydraulic servo rock triaxial test system that can render real-time stress-strain curve and using the contact deformation of high-precision acquisition extensometer. The SH-II all-weather health monitoring system is produced by Physical Acoustics Company; the system can simultaneously get 16 channels' real-time acquisition AE signal, and it can collect the flow waveform and store it in the signal storage drive for repeating the analysis. The system is also equipped

with waveform analysis and postprocessing software for analyzing the main AE parameters, such as the count, amplitude, energy, and events. BSJ-A automatic vacuum water-full testing machine is used as the water-filling equipment. The rock mechanics experimental system is shown in Figure 2.

2.3. The Experimental Process. Before the test, the sample is divided into two groups: one group is dried by heating for 24 hours so that the sample does not contain water and the other group is filled with full water for 24 hours using the vacuum water-filling machine. Dry sample and water-full sample are used, respectively, for splitting and uniaxial compression AE experiment, the diameter and the length are measured after inputting information into the computer, and the experiment process uses 0.05 kN/s displacement control load through the feedback information of plot stress-strain curve. To monitor the sample destruction of the whole process of AE, the simulation filter is set between 20 kHz and 1 MHz and the sampling frequency is set at 1 MHz. Uniaxial compression uses four Nano 30 sensors that are fixed on both ends of the specimen, and splitting uses two Nano 30 sensors to probe on the side of the specimen (as shown in Figure 3); the specimen-sensor interface was painted with an coupling agent. To exclude the outside noise signal as far as possible, the AE threshold is set to 40 dB and the pre-amplifier gain modulation is set to 40 dB. Compression experiment is continued by loading until the sample breaks. To ensure the coupling effect and the positioning accuracy of the sensor, first, the sample is fixed in the set position by using an elastic belt and a coupling agent, and then, the broken lead method is used to determine the coupling and connectivity of sensors near each sensor. Afterwards, the AE automatic test system is used to obtain the receiving matrix of each sensor after transmitting the standard waveforms. The coupling effect is judged by the amplitude of AE. If the amplitude is greater than 90 dB, then it is considered that the coupling effect is better. At the same time, the average velocity of AE is 3850 m/s, and it is used as the location.

2.4. Energy Calculation Method. In the respect of doing work, the distance passed in the direction of the force is the work, and the process of providing force to the rock sample is also the work of the rock sample, which leads to the damage of the rock sample (Figure 4). Essentially, it is a kind of energy transfer and transformation. Compression provides energy to the rock sample, and energy release occurs when the rock sample reaches the limit state of energy storage. The released and accumulated energy is calculated using the following formula:

$$W_i = (P_2 - P_1) * (m_2 - m_1),$$
$$W = \sum_{i=0}^{i=m_N} W_i, \quad (1)$$

where W_i is the energy at a certain time and W is the energy accumulated. The corresponding loads and displacements of P and m are measured in kN and mm, respectively.

3. Analysis of the Experiment Results

3.1. Tensile Strength and Softening Coefficient Analysis. There are many theories and results on rock uniaxial compression, but less research studies on tensile characteristics, the essence of rock tension damage on macro controls the stability of rock engineering. The results of tensile damage of basalt columnar joints are shown in Table 1, the tensile strength curve is shown in Figure 5, and the tensile failure pattern and failure surface are shown in Figure 6.

From Figures 5(a) and 5(b), we can see that the saturated state splitting declining curve peak period has a certain radius than the drier conditions and the saturated rock energy release rate is slower than that of the dry rock; thus, it is shown that the rock is affected by the water viscosity. From Table 1, it can be seen that the dry sample tensile strength ranged between 6.330 and 6.982 MPa, with an average of 6.657 MPa, and the results have small discrete, the discrete rate ranges between 0.27 and 4.91%; the saturated rock strength ranges between 4.178 and 4.835 MPa, with an average of 4.505 MPa, and the discrete rate is in the range of 0.64~7.32%. The saturated specimen has more irregularity obvious than the dry specimen. The strength of saturated specimens is 2.152 MPa lower than that of dry specimens, and the softening coefficient is 0.68. The surface of the splitting basalt columnar joints shows not only a large number of small structural planes but also a large number of microcracks in it.

When Brazilian splitting method is used to stretch rock samples, mechanical energy is transferred by triangular knife edge. The degree of knife edge sharpness is related to the amount of accumulated energy in the contact area of rock samples, and the degree of contact surface and knife edge closeness has an effect on the tensile strength. And the degree of the cut blade affects the tensile strength. From the failure process, the crack in all samples first appears at the edge of high stress. Along with it external load continues to provide energy, the rock sample damages in half under the action of shear force and tension specimen. Most dry samples' split surfaces follow the baseline craze. Most of the splitting surfaces of dry rock samples crack along the baseline. The splitting surface of saturated rock samples cracks from upper and lower cutters, but seldom along the baseline. The main reason is that after saturated water of columnar jointed basalt, some strong planes are converted into weak planes under the physical and chemical action of water, which enhances the discreteness of rock samples. The crisp sound of drying rock sample of columnar jointed basalt occurs at the moment of splitting. The main reason is that more energy is accumulated in the drying sample, which is released instantaneously. The energy stored in the saturated sample is less, and the sound is not obvious when the sample is broken.

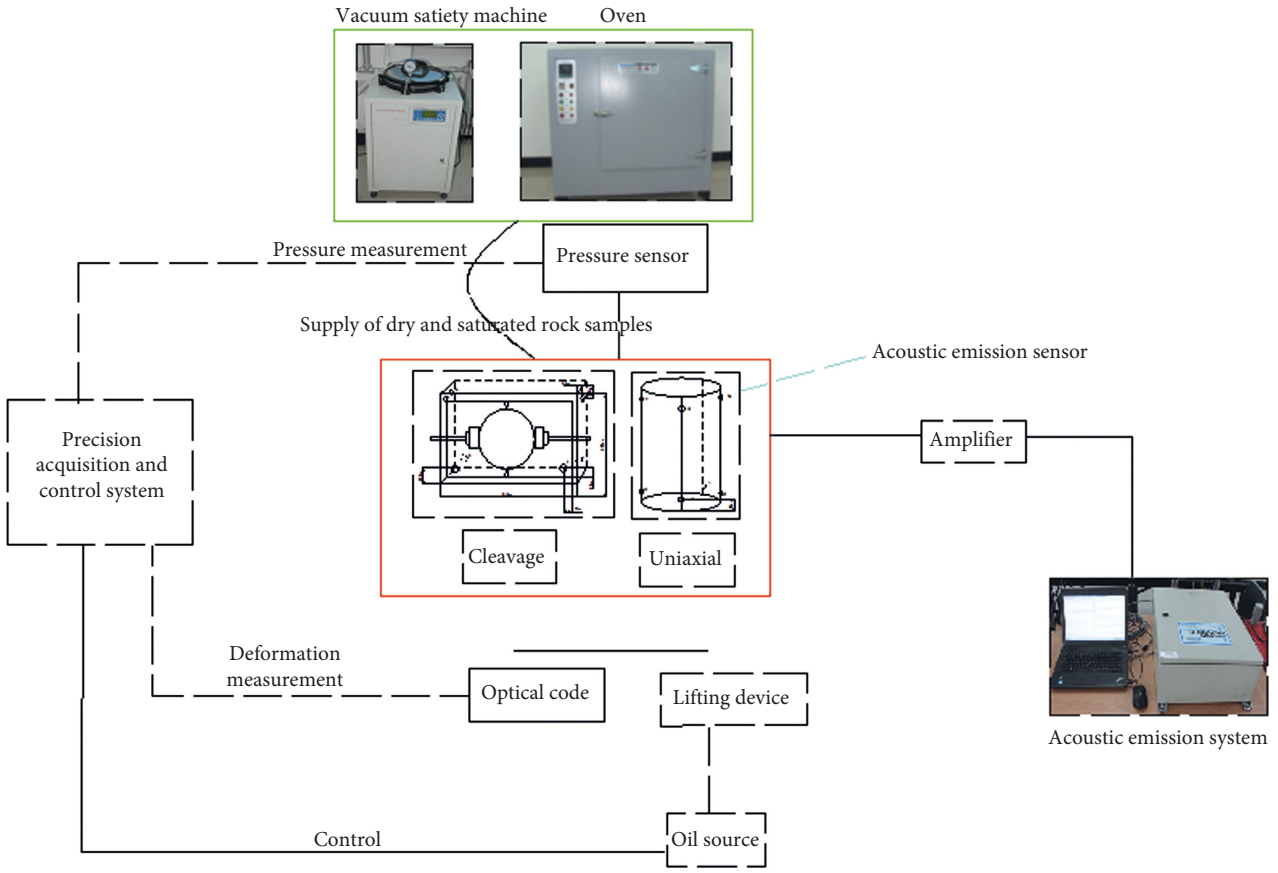

Figure 2: Rock mechanics experimental system.

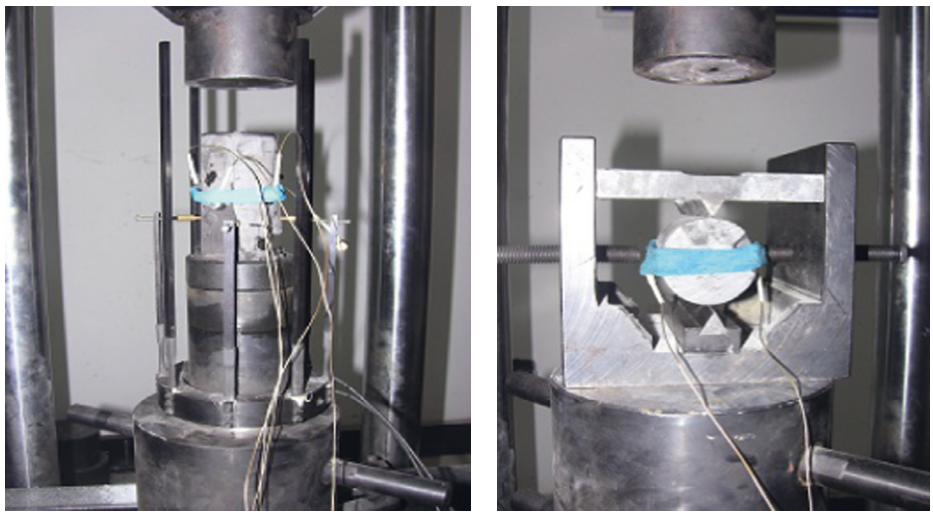

(a) (b)

Figure 3: Splitting experiment and uniaxial compression: (a) uniaxial AE test and (b) shear AE test.

3.2. Uniaxial Compressive Strength and Softening Coefficient Analysis. The rock stress-strain curve reflects the true failure process. It reflects the rock-bearing capacity, and a study on rock mechanics properties is one of the important basic ways to evaluate the stability of rock engineering. Uniaxial compressive strength of basalt columnar joints is shown in Table 2, and the typical failure pattern is shown in Figure 7.

According to the results in Table 2, the basalt columnar joints has certain discrete, because it has a large number of joints and fissures. Compressive strength of dry state ranges

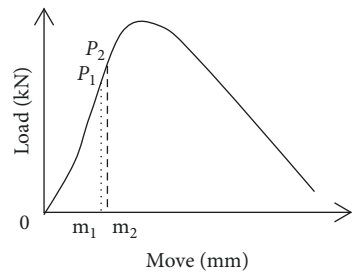

Figure 4: Schematic diagram of energy calculation.

Table 1: Basalt columnar joints and tensile strength of the sheet.

Moisture condition	Specimen number	Sample size: diameter × height (mm)	Breaking load (kN)	Tensile strength (MPa)	Average value (MPa)	Energy (kN × mm)	Average value (kN × mm)
Saturation	Pb-1	φ50.2 × 27.1	9.487	4.440	4.505	217.673	221.008
	Pb-2	φ50.3 × 18.4	9.827	4.595		234.529	
	Pb-3	φ50.3 × 25.5	8.447	4.178		210.903	
	pb-4	φ50.3 × 20.1	7.128	4.476		213.481	
	pb-5	φ50.2 × 14.8	5.668	4.835		228.453	
Dry	pg-1	φ50.3 × 25.3	13.386	6.675	6.657	239.891	242.401
	pg-2	φ50.3 × 22.7	11.485	6.404		246.444	
	pg-3	φ50.2 × 18.8	9.381	6.330		242.405	
	pg-4	φ50.3 × 27.3	15.085	6.982		239.902	
	pg-5	φ50.5 × 15.0	8.247	6.895		243.364	

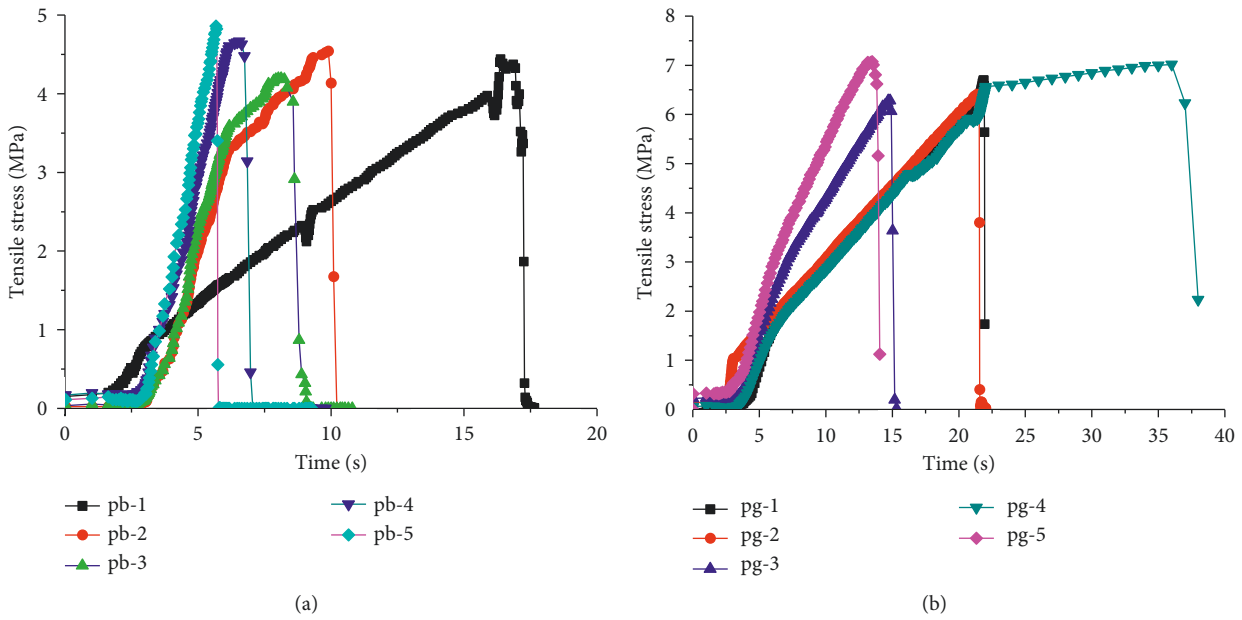

Figure 5: Splitting curve of the (a) saturated specimen and (b) dry specimen.

between 115.509 and 130.481, with an average of 122.405 MPa, and the discrete rate ranges between 0.11 and 6.60%. Compressive strength of saturated state ranges between 74.727 and 109.518, with an average of 95.172 MPa, and the discrete rate ranges between 1.68 and 21.48%. The discreteness of saturated sample is larger than that of the dry sample, which indicates that water aggravates irregularity of basalt columnar joints leading to more complexing columnar joints of mechanical properties. After water saturation, the strength of basalt decreases by 27.233 MPa and the softening coefficient is 0.78. Water has some influence on the strength of columnar jointed basalt.

The strength of the basalt columnar joints is much higher than that of other types of rock. The process of loading stores a large amount of elastic energy, the rock damage instantly produces a loud noise, and a large number of small blocks burst. In order to analyze its failure characteristics, the basic shape of the rock is preserved by external wrapping with the

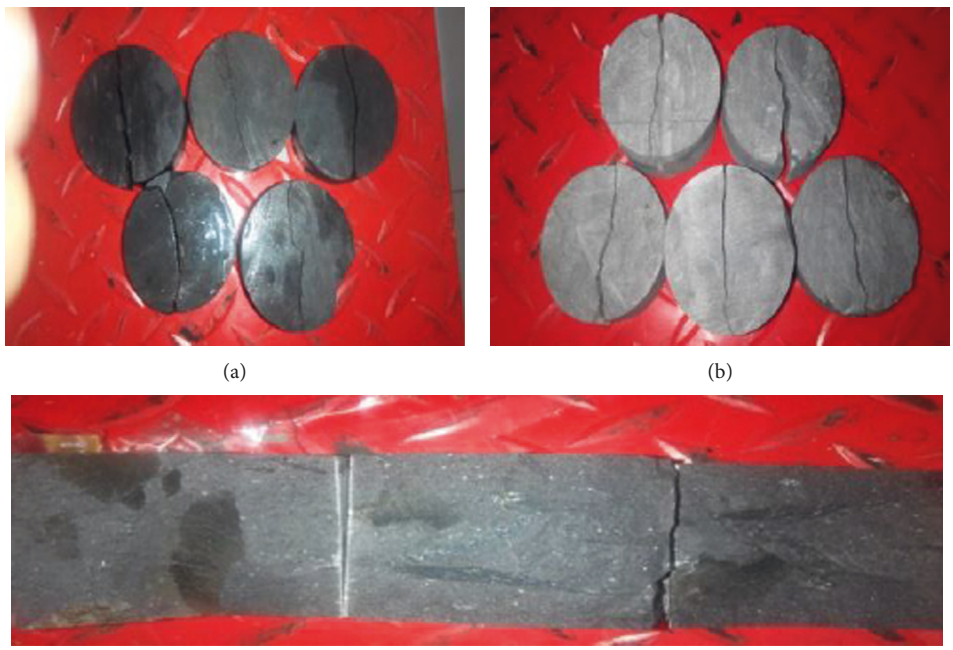

(a) (b)

(c)

Figure 6: Fracture morphology of columnar jointed basalt under tension.

Table 2: The uniaxial compressive strength.

Moisture condition	Number	Diameter (m)	Length (m)	Fracture load (kN)	Compressive strength (MPa)
Saturated	db-1	50.38	100.42	177.519	89.051
	db-2	50.45	101.12	218.927	109.518
	db-3	50.67	101.05	150.685	74.727
	db-4	50.62	100.74	212.904	105.791
	db-5	50.55	100.84	194.212	96.771
Dry	dg-1	50.76	100.36	237.522	117.374
	dg-2	50.49	100.47	252.518	126.122
	dg-3	50.37	101.22	260.004	130.481
	dg-4	49.96	100.34	240.217	122.537
	dg-5	50.48	100.32	231.178	115.509

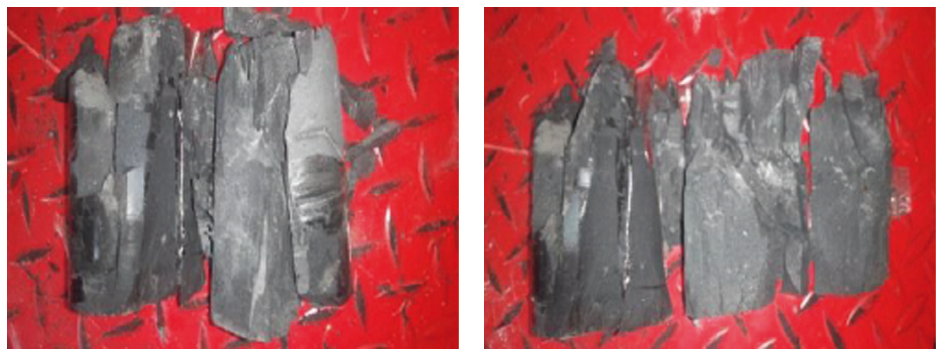

(a) (b)

Figure 7: Typical failure pattern.

tape. Longitudinal splitting is a typical damaging pattern, that is, the rock breaks perpendicular to the direction of the axial load, and a large number of microcracks break into small pieces. From the cross section, we can find internal multilayer and multiple fractures. The stress-strain curve indicates that this kind of yield stages of rock failure is not obvious in the process, and the damage is instantaneous, which is hard to predict fracture difficulty.

3.3. Splitting Rock AE Characteristics. The AE characteristic curve of the splitting dry and saturated basalt columnar joints is shown in Figures 8 and 9, respectively.

Figure 8 shows changes in dry rock fracturing with respect to AE parameters. Figure 8(c) the load is zero in the 0~2 s, AE activities thimbleful in 2–4 s period, the load suddenly increases, the sample is densification phase, Figure 8(b) AE energy is almost zero, Figures 8(a) and 8(c) AE of amplitude and count number increases instantaneously. The load increases uniformly in the 4–22 s period. The count and amplitude of AE increase steadily with the uniform increase of load. From Figure 8(d), it can be seen that the energy is less than 7000, the amplitude is less than 850 dB, and the amplitude and energy of AE are inversely proportional. In the period of 22-23 s, it can be seen from Figure 8(d) that the load has been reduced to zero and the specimen has been destroyed. At this time, there are many high-energy AE events. The total energy of AE instantaneously increases to the maximum, while the amplitude and count rate of AE show a downward trend. Through the above process, it can be concluded that the energy, amplitude, and load of AE show a positive trend. Relatively, the rock sample destroys instantaneously and releases a lot of energy. Figure 9 shows AE parameter changes under saturation state splitting. Figure 9(c) shows that the load is zero in the 0~2 s period, and the AE signal barely increases. The overall load rises in the 2–17 s period, because the microcracks accumulate to a certain degree to extend the big crack which causes the curve middle to load back twice. In Figures 9(a)–9(c), AE amplitude, energy, and count show an increasing trend, but compared with the dry sample, amplitude and count value are small and have more fluctuations, the energy value is very small, and change is not obvious. In Figure 9(d), it can be seen that from energy within 4000 aJ and amplitude within 450 dB, the greater amplitude corresponds to the lower energy, and it represents a triangle trend. High amplitude counts appear at this time, and the count number reaches the peak, but the count and amplitude ratio shows a trend of decline. From the aforementioned process, it can be seen that AE energy and amplitude with load show the same trend, AE energy lags, and the dry sample has similar results. At the initial load stage, the protogenesis fracture closes with the AE signal when new crack extension leads to the specimen's AE activity. When break reduces the AE activities, the rock sample has low energy before the sample destruction, and the destruction instantly reaches to the biggest.

By comparing the AE activity in the splitting process, it is found that the AE activity in the dry state is more active than that in the saturated state. The more the AE count is, the larger the energy is, and the more the count of high amplitude is, smaller the fluctuation of parameters is. The dry sample collects about 1258 AE signal counts and energy is 190004 aJ, and the saturated sample collects 675 AE signal counts and energy is 61080 aJ.

3.4. Typical AE Characteristics of Rock under Uniaxial Compression. Each sample collection curve is similar, and only typical curves are selected for analysis. Figure 10 shows the AE characteristic curves of dry basalt columnar joints under uniaxial compression, and Figure 11 shows AE characteristic curves of saturated basalt columnar joints under uniaxial compression.

Figure 10 shows the dry rock failure process of AE parameters with respect to time. It is evident that basalt columnar joints conform to the four stages of general rock breaking (Figure 10(b)), and they are the compaction stage, elastic stage, plastic stage, and remnant stage. Figures 10(a) and 10(b) show that the count and amplitude have high speed growth, but the energy has been in a smaller value in 0~70 s, and the early loading AE activity shows sample internal fissures changed under low load. Figure 10(c) shows that 12 AE events occurred and show scattered distribution. Figure 10(d) shows that the energy is less than 10,000 and the amplitude is less than 5,000 dB, but the amplitude of AE is inversely proportional to the energy, and they show a triangular relationship. Amplitude and count start to decrease and then increase; the energy rapidly increases to peak after stability in 70~90 s, and high-energy count reach to 65000. The total events produced were 38, and the overall distribution is irregular, which explains the rock internal flaw complexity. When the load increases to 85% failure load, amplitude and count rate reach to trough low ebb area, but a large number of high-energy counts appear. With the increase of load, plastic deformation and failure occur in rock samples. At the time of damage, the amplitude and cumulative counting curve of AE increase by leaps.

Figure 11 shows the AE characteristics of saturated rock failure process; from Figure 11(b), we can see the change of stress and strain in the whole process of rock sample failure. AE count and amplitude decreases in 0~40 s, and energy is almost zero. Figures 11(a) and 11(b) show that the count and amplitude increase at a constant rate and energy raises at a slower speed rate in 40~125 s. The count and amplitude start to increase and then decrease within the scope of 125~157 s, a large number of count with an amplitude greater than 5000 dB occurred, and energy rapidly reaches a maximum. Amplitude and energy present triangle relation; a total of 34 AE events appears, but they exist disorderly. The rock whole failure process and the AE activities are related: in the initial loading pressure stage, primary cracks and voids closure phenomenon occur, which releases certain energy and thus AE activities appear. When the load reaches the elastic stage, only a small amount of energy is released and thus the AE activity occurs less. Densification stage and elastic stage show weak AE activity; hence, some scholars call this period as the blank period. After entering the plastic period, the new crack initiation and propagation releases large amounts of energy, and the AE activity becomes active. When the destruction of the rock sample occurs, a large number of cracks appear and it becomes a macrocrack; the AE activity reaches the peak at this time. It can be found from the above analysis that there is an obvious period before the destruction of the dry basalt columnar joints; an obvious densification stage exists in the saturated sample, but the rock destruction in the blank period is inconspicuous. Dry sample density is larger and

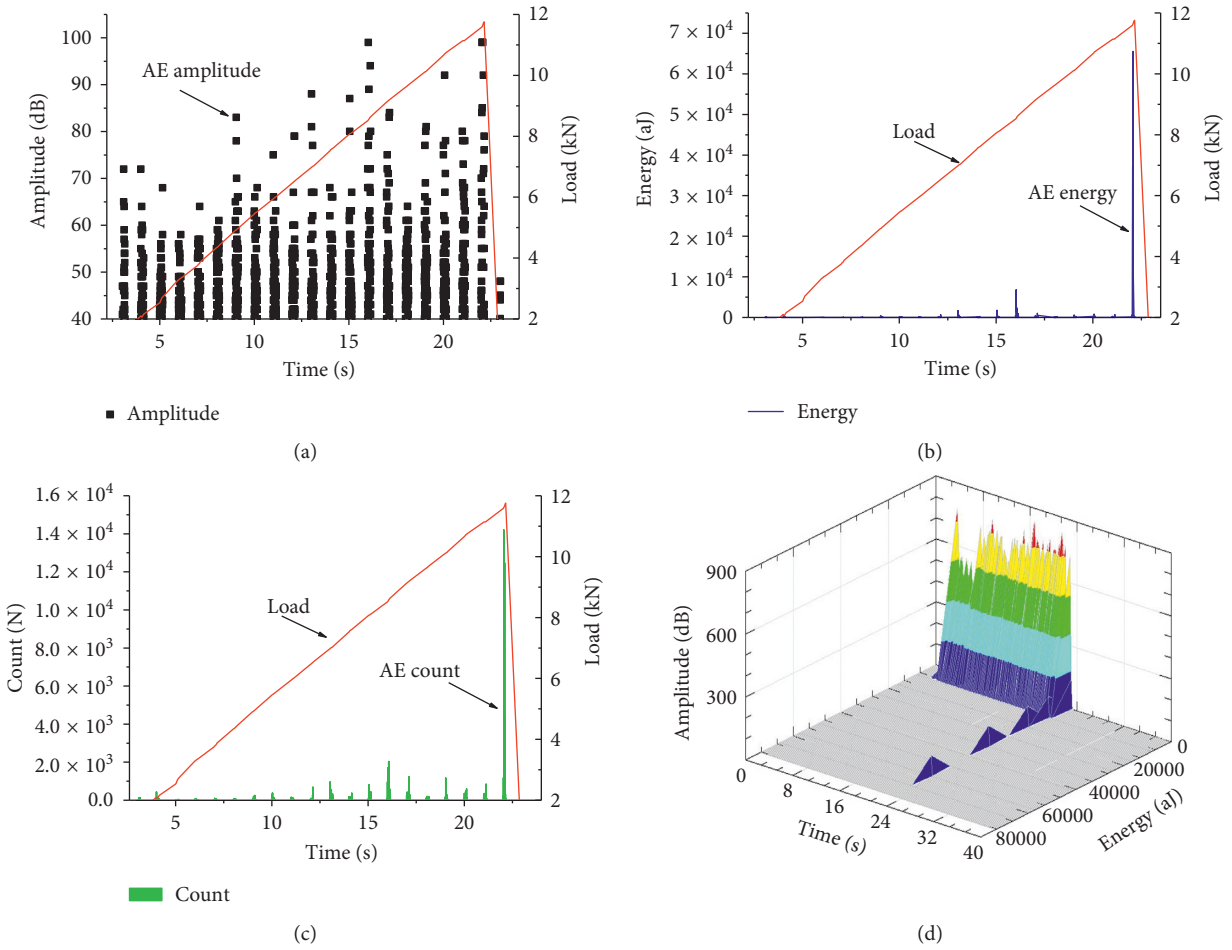

Figure 8: AE characteristics of the basalt columnar joints under dry state: (a) AE amplitude and time, (b) AE energy and time, (c) AE count and time, and (d) AE amplitude, energy, and time.

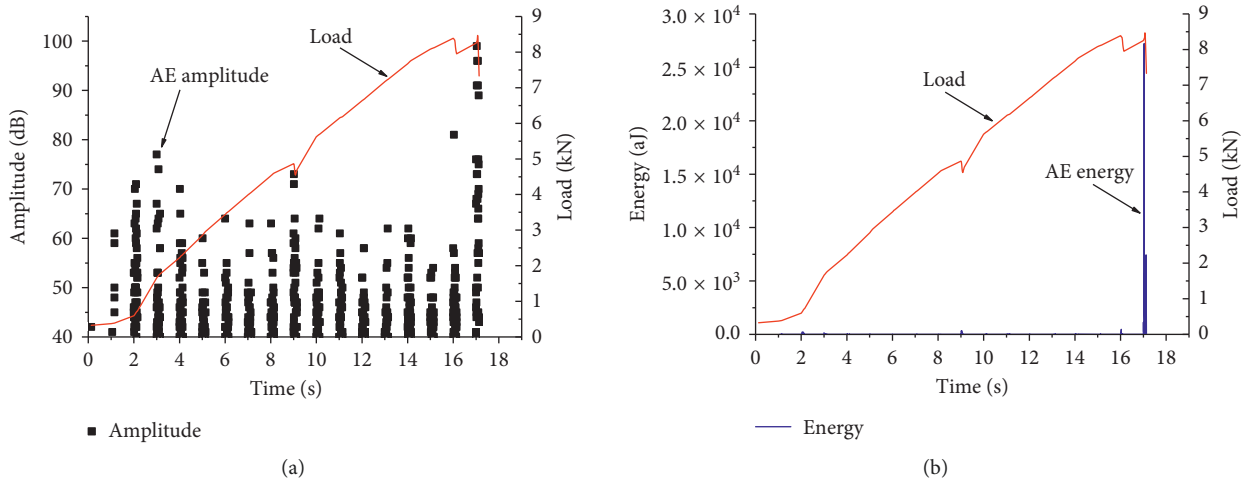

Figure 9: Continued.

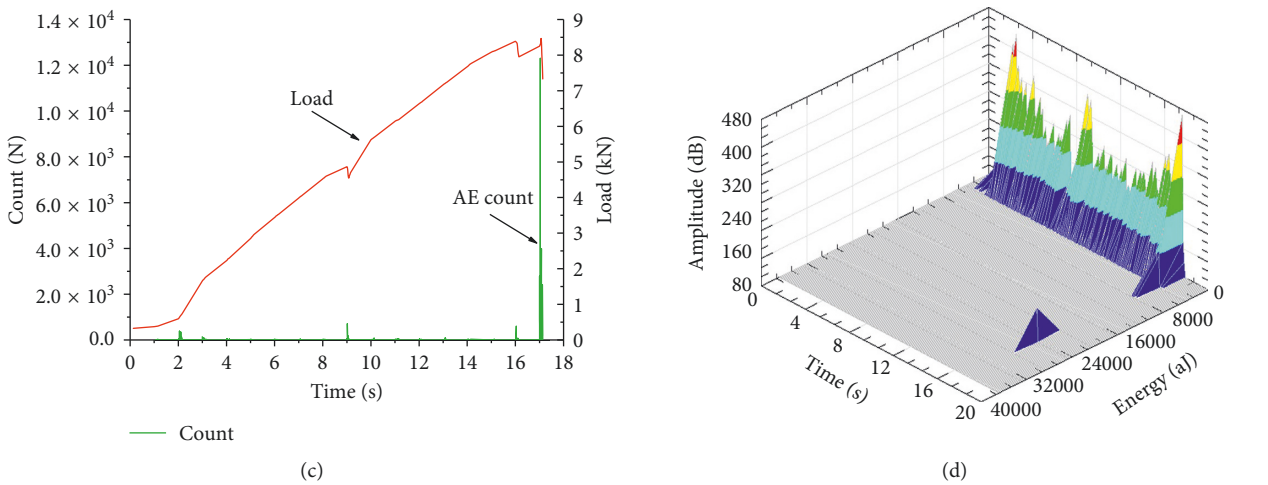

Figure 9: AE characteristics of the basalt columnar joints under saturated state: (a) AE amplitude and time, (b) AE energy and time, (c) AE count and time, and (d) AE amplitude, energy, and time.

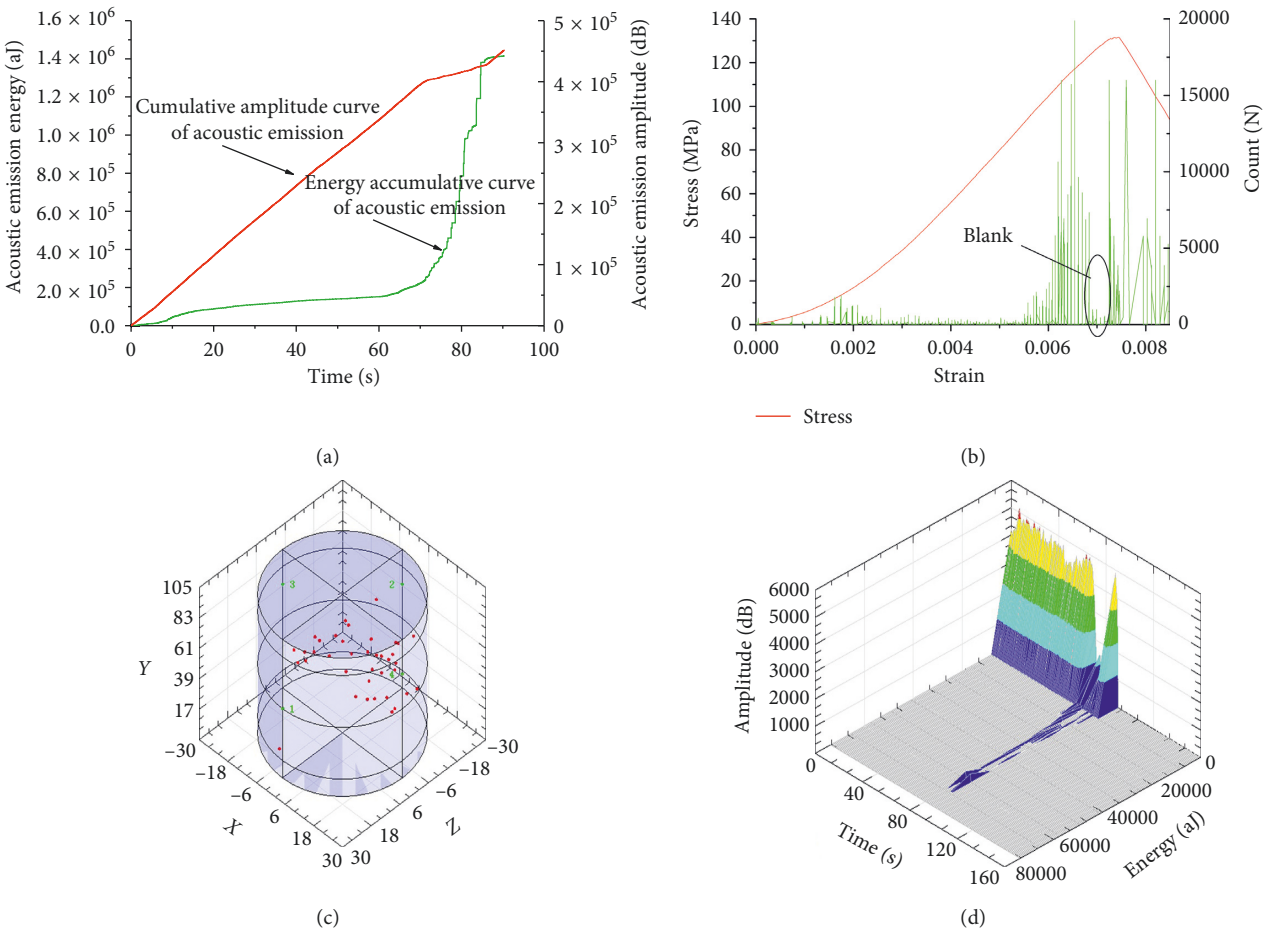

Figure 10: AE characteristics of basalt columnar joints of dry state under uniaxial compression: (a) AE amplitude and AE energy time, (b) AE count and time, (c) AE location, and (d) AE amplitude, energy, and time.

the internal is close-grained, its densification stage is not obvious, and the saturated rock starts to swell because water has an effect, so there is an obvious pressure dense phase.

3.5. Analysis of Uniaxial Compression and Splitting AE Experiment Results. We find that uniaxial compression and splitting the AE activities have their own characteristics by experiment, but there is also a certain relationship. A large

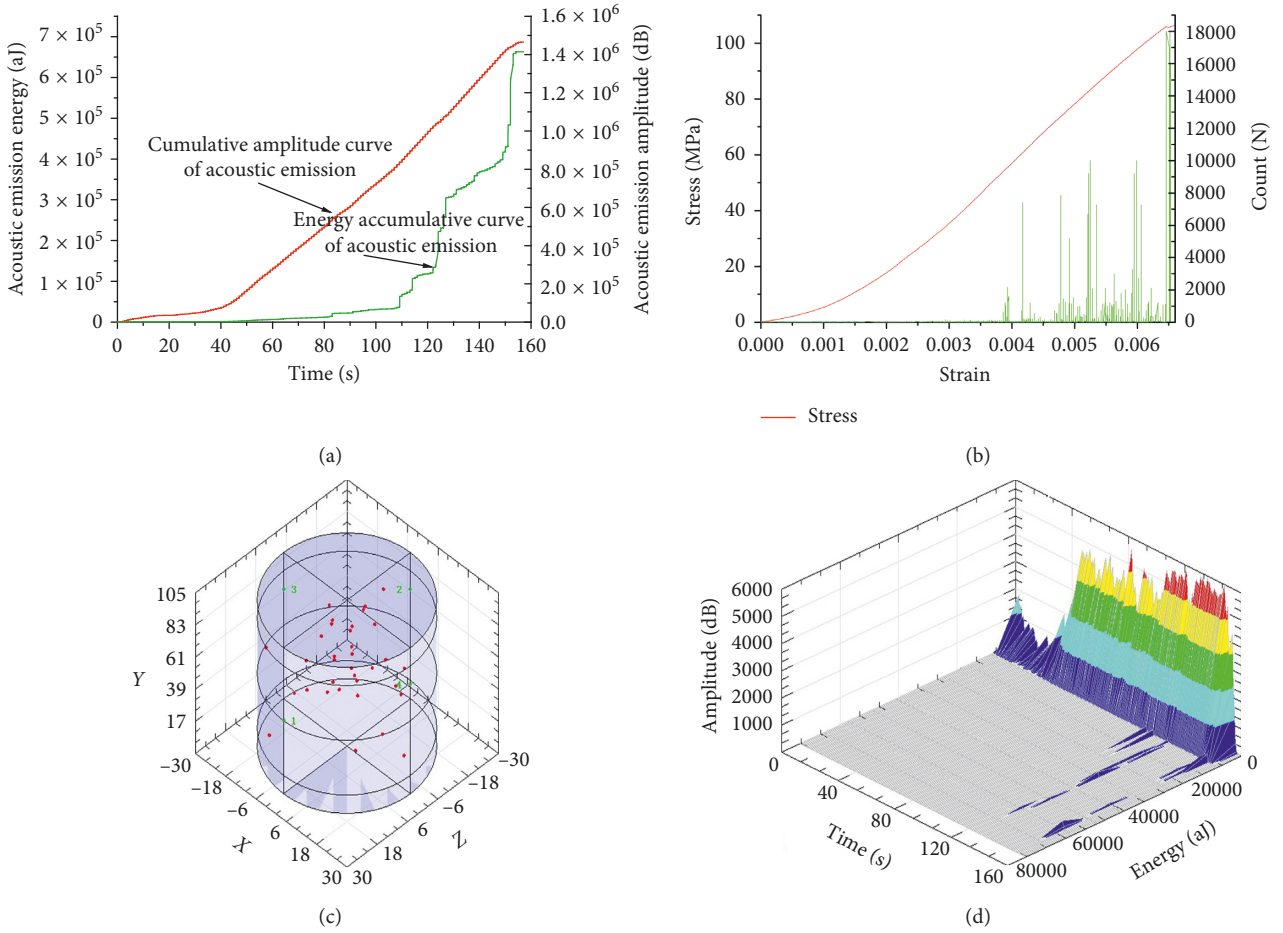

Figure 11: AE characteristics of basalt columnar joint of saturated state under uniaxial compression: (a) AE amplitude and AE energy time, (b) AE count and time, (c) AE location, and (d) AE amplitude, energy, and time.

number of AE signals appear at the early stage of the dry sample uniaxial compression. It is similar to the early splitting AE characteristics. A large number of AE signals appear at the later stage of the saturated rock uniaxial compression. It is similar to late splitting AE characteristics. In saturated rock uniaxial compression, exists densification stage, but in dry sample uniaxial compression and splitting experiment, densification stage is not obvious. When the dry rock sample is close to failure, in the AE appears blank period, but there is no AE blank period in saturated rock samples and splitting experiments.

Uniaxial compression and splitting experiment process show approximately the same AE characteristics. The densification stage produces less AE signal, the elastic stage turns to be active, and the plastic phase is very active. Energy has increased dramatically when it is close to the breaking load. Splitting failure is caused by the combined action of tensile stress and compressive stress; there is stress concentration at the edge of upper and lower end face, so the failure mode is different from the principle. Compared to uniaxial compression, splitting needs less energy to make rock damage, and AE activity and energy are small. AE amplitude is higher corresponding to the lower energy and the count is less; thus, it shows an obvious triangle relation. The AE location result disorder shows the rock complex.

Crack stability extent, rapid extent, and cut-through every stage of AE activity increased step by step. During the whole process of rock sample loading to failure, the AE activity and the propagation of microcracks in the rock sample show a unified law, and AE dynamic also reflects the law of rock sample. The results of uniaxial and splitting experiments show that the energy-time columnar accumulative maps only occur in the failure stage, and the energy of columnar jointed basalts in the early stage of failure is very low, even neglected. As a result, the AE damage uses energy variation expression that is more correct and more suitable for prediction criterion.

4. Conclusion

This paper studies on the saturated basalt columnar joints and dry basalt columnar joints under uniaxial compression fracture process AE law. Through the contrast analysis of AE parameters and characteristics of failure process for basalt columnar joints, damage prediction provides certain guidance:

(1) It indicates that water increases the irregularity of basalt columnar joints. This result shows that water weakens basalt columnar joints' strength. There are many beds and fissures in the columnar jointed basalt, and heterogeneity is more complicated than other rocks.

(2) Under uniaxial compression, in the dry basalt columnar joints, the AE appears in the blank period before destruction. It can be used as early signs of instability. The saturated basalt columnar joints have an obvious pressure dense stage that produces a small number of AE signals.

(3) It can be found from the results of the uniaxial compression and fracturing process experiment that similarities exists in the AE law, but there are also differences in local. As splitting is the combination of tension and compression and stress concentrate exists at the edge, compared with the uniaxial compression, the AE of total energy and activity is weak. It is mainly due to the differences in two kinds of the failure mechanism.

(4) From the amplitude-events-energy diagram, it can be found that with the increase of amplitude, the corresponding count and energy decrease, presenting obvious triangles. From the AE location map of uniaxial compression failure, it can be found that the AE events are disordered and scattered in various regions, which is consistent with the result that rock samples are destroyed into a large number of small blocks.

(5) The study of uniaxial compression and splitting AE phenomenon found that the columnar jointed basalt is in the process of loading to the early stage, AE energy is very low even negligible, and the sample damage occurs at high-energy concentration. Therefore, it is more believable to judge stability from the energy than from the high count.

Data Availability

The data used to support the findings of this study are included within the article.

Conflicts of Interest

The authors declare that they have no conflicts of interest.

Acknowledgments

This research was supported by the National Natural Science Foundation of China (51574115, 51574006, 51674107, 51774121, 51604100, and 51674109). The authors would like to thank all members for their help with the field work in Heilongjiang Ground Pressure & Gas Control in Deep Mining Key Lab (GPGC).

References

[1] Y.-H. Li, J.-P. Liu, X.-D. Zhao, and Y.-J. Yang, "Study on b-value and fractal dimension of acoustic emission during rock failure process," *Rock and Soil Mechanics*, vol. 30, no. 9, pp. 2559–2574, 2009.

[2] Y.-B. Zhang, X.-H. Huang, S.-S. Li, and X.-X. Liu, "Spectral character analysis of sandstone under saturation condition in rupture procedure," *Rock and Soil Mechanics*, vol. 34, no. 6, pp. 1574–1578, 2013.

[3] B. Liu, J. Huang, Z. Wang, and L. Liu, "Study on damage evolution and acoustic emission character of coal-rock under uniaxial compression," *Chinese Journal of Rock Mechanics and Engineering*, vol. 28, no. 1, pp. 3234–3238, 2009.

[4] K. Zhao, J.-F. Jin, X.-J. Wang, and K. Zhao, "Study on rock damage and acoustic emission based on ultrasonic velocity test of rock specimen under uniaxial compression," *Rock and Soil Mechanics*, vol. 28, no. 10, pp. 2105–2110, 2007.

[5] X. Yu, Q. Xie, X. Li, Q. Wang, and Z. Song, "Acoustic emission of rocks under direct tension, brazilian and uniaxial compression," *Chinese Journal of Rock Mechanics and Engineering*, vol. 26, no. 1, pp. 137–142, 2007.

[6] Z.-T. Zhang, J.-F. Liu, L. Wang, H.-T. Yang, and R. Zhang, "Mechanical properties and acoustic emission characteristics of coal under direct tensile loading conditions," *Journal of China Coal Society*, vol. 38, no. 6, pp. 960–965, 2013.

[7] N. Li, Z.-Y. Sun, D.-Z. Song, and M.-Y. Jin, "Experimental study on acoustic emission characteristic of raw coal failure under splitting test and uniaxial compression," *Coal Safe*, vol. 10, pp. 45–48, 2013.

[8] J.-H. Fu, B.-X. Huang, C.-Y. Liu, W. Yang, and L.-F. Wang, "Study on acoustic emission features of coal sample brazilian splitting," *Coal Science and Technology*, vol. 39, no. 4, pp. 25–28, 2011.

[9] X.-M. Li, B.-X. Huang, C.-Y. Liu, X. Wang, and F. Liu, "Study on acoustic emission characteristics of mould coal under compression-shear conditions," *Journal of Hunan University of Science and Technology*, vol. 25, no. 1, pp. 22–26, 2010.

[10] F.-K. Xiao, G. Liu, H.-Q. Fan, and X.-L. Meng, "Test of acoustic emission characteristic of coal-body failure in methane drainage bore-hole," *Coal Mining Technology*, vol. 18, no. 2, pp. 7–10, 2013.

[11] F. Xiao, H. Fan, G. Liu, and X. Meng, "Study of acoustic emission characteristics of coal containing gas under triaxial compression," *Journal of Heilongjiang Institute of Science and Technology*, vol. 23, no. 1, pp. 10–15, 2013.

[12] Z. Zhengwen, M. Jin, and L. Liqiang, "AE b-value dynamic features during rockmass fracturing and their significance," *Seismology and Geology*, vol. 1, no. 17, pp. 7–11, 1995.

[13] S. Zhang, J. Liu, C. Shi, Y. Li, X. Zhao, and Y. Yang, "Study on precursory characteristics of rock failure based on acoustic emission experiment," *Metalmine*, vol. 386, no. 8, pp. 65–68, 2008.

[14] C. Tang, H. Qiao, and X. Xu, "Numerical simulation on pillar failure and associated acoustic emissions," *Journal of China Coal Society*, vol. 1, no. 23, pp. 266–269, 1999.

[15] G. Wu and Z. Zhao, "Acoustic emission character of rock materials failure during various stress states," *Chinese Journal of Geotechnical Engineering*, vol. 20, no. 2, pp. 82–85, 1998.

[16] Z.-P. Meng, "Experimental research on acoustic wave velocity of coal measures rocks and its influencing factors," *Journal of Mining and Safety Engineering*, vol. 22, no. 3, pp. 18–27, 2008.

[17] J. Chu, *Acoustic Emission Prediction of Rock Fracture and Application to Geostress Survey of Kaiser Effect*, Shandong University of Science and Technology, Qingdao, China, 2008.
[18] N. Dixon and M. Spriggs, "Quantification of slope displacement rates using acoustic emission monitoring," *Canadian Geotechnical Journal*, vol. 44, no. 8, pp. 966–976, 2007.
[19] D. Arosio, L. Longoni, M. Papini, M. Scaioni, L. Zanzi, and M. Alba, "Towards rockfall forecasting through observing deformations and listening to microseismic emissions," *Natural Hazards and Earth System Science*, vol. 9, no. 4, pp. 1119–1131, 2009.
[20] Z. Liang, X. Liu, Y. Zhang, and C. Tang, "Analysis of precursors prior to rock burst in granite tunnel using acoustic emission and far infrared monitoring," *Mathematical Problems in Engineering*, vol. 2013, Article ID 214340, 10 pages, 2013.
[21] F. Xiao, G. Liu, Z. Zhang, Z. Shen, F. Zhang, and Y. Wang, "Acoustic emission characteristics and stress release rate of coal samples in different dynamic destruction time," *International Journal of Mining Science and Technology*, vol. 26, no. 06, pp. 981–988, 2016.
[22] GB/T23561.7, *Coal and Rock Physical and Mechanical Properties Determination Method*, China Standard Publishing, Beijing, China, 2009.